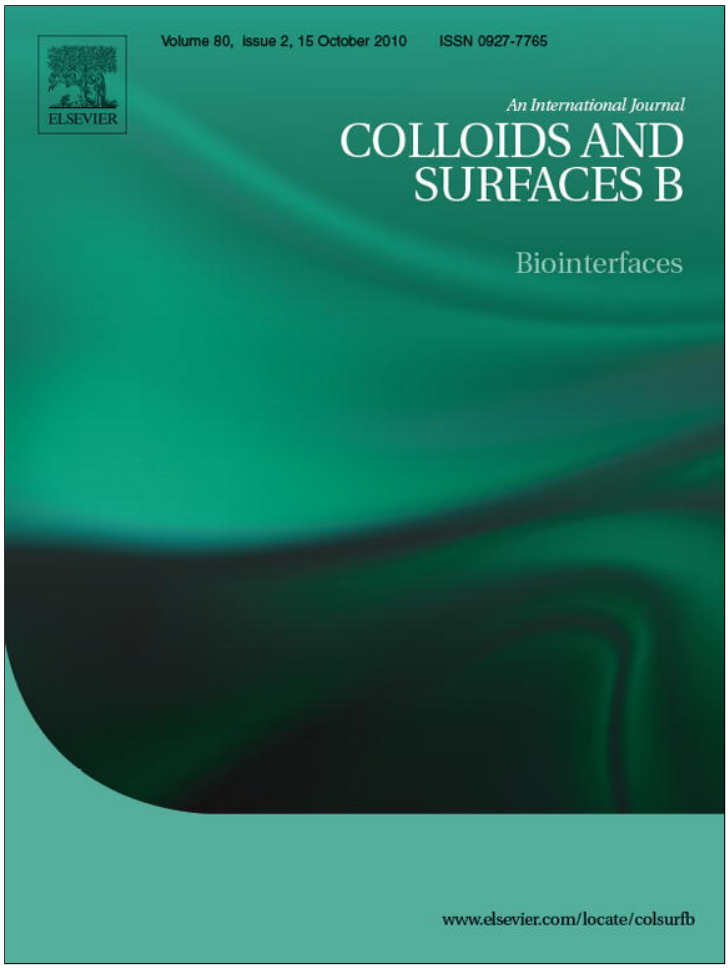

Colloids and Surfaces B: Biointerfaces 80 (2010) 219–226

Contents lists available at ScienceDirect

Colloids and Surfaces B: Biointerfaces

journal homepage: www.elsevier.com/locate/colsurfb

Morphological changes of supported lipid bilayers induced by lysozyme: Planar domain formation vs. multilayer stacking

Valeriya M. Trusova[a,*], Galyna P. Gorbenko[a], Irina Akopova[c], Julian G. Molotkovsky[b], Ignacy Gryczynski[c,d], Julian Borejdo[c], Zygmunt Gryczynski[c]

[a] Department of Biological and Medical Physics, V.N. Karazin Kharkov National University, 4 Svobody Sq., Kharkov 61077, Ukraine
[b] Shemyakin-Ovchinnikov Institute of Bioorganic Chemistry, Russian Academy of Sciences, 16/10 Miklukho-Maklaya, Moscow 117871, Russia
[c] Department of Molecular Biology and Immunology, University of North Texas Health Science Center, 3500 Camp Bowie Blvd., Fort Worth 76107, TX, USA
[d] Department of Cell Biology and Genetics, University of North Texas Health Science Center, 3500 Camp Bowie Blvd., Fort Worth 76107, TX, USA

ARTICLE INFO

Article history:
Received 30 May 2010
Received in revised form 10 June 2010
Accepted 16 June 2010
Available online 25 June 2010

Keywords:
Lysozyme
Supported lipid bilayers
Lipid demixing
Multilayer stacks

ABSTRACT

Total internal reflection fluorescence microscopy (TIRFM) has been utilized to explore the effect of cationic protein lysozyme (Lz) on the morphology of solid-supported lipid bilayers (SLBs) comprised of zwitterionic lipid phosphatidylcholine (PC) and its mixture with anionic lipid cardiolipin (CL). Kinetic TIRFM imaging of different systems revealed subtle interplay between lipid lateral segregation accompanied by exchange of neutral and acidic lipids in the protein–lipid interaction zone, and the formation of lipid multilayer stacks. The switch between these states was shown to be controlled by CL content. In weakly charged SLBs containing 5 mol% CL, assembling of CL molecules into planar domains upon Lz adsorption has been observed while at higher content of anionic lipid (25 mol%) in-plane domains tend to transform into multilayer stacks, thereby ensuring the most thermodynamically-favorable membrane conformation.

1. Introduction

The early 1970s have been marked with the development of revolutionary Singer and Nicholson fluid mosaic model envisioning biological membrane as two-dimensional solution of proteins uniformly distributed in homogeneous lipid media [1]. During the next decades, however, this conceptualization has been replaced by the idea of lateral heterogeneity of membrane components. A plethora of results from both theoretical and experimental studies provided indisputable evidence for existence of highly dynamic membrane domains housing specific lipids and proteins [2–5]. These supramolecular assemblies are usually considered as spatially limited membrane areas distinguished from their neighboring regions by one or more measurable properties, e.g., molecular order and dynamics [2]. The driving force for membrane compartmentalization was shown to involve lipid–lipid, lipid–protein, and protein–protein interactions, osmotic pressure and temperature change, physiological stimuli, etc. [6–9]. One class of lipid inhomogeneities, currently getting the growing attention, is represented by the domains formed by acidic lipids in respond to adsorption of oppositely charged cationic proteins [10–12]. Such sequestration is usually explained by the tendency of lipids to minimize the electrostatic free energy of protein–lipid binding. More specifically, in a binary membrane system proteins perform lipid sorting in such a way that those anionic lipid species, possessing the highest affinity for the polypeptide due to strong electrostatic interactions, would be crowding around the protein. These membrane domains rich in protein and anionic lipids coexist with protein-free neutral lipid assemblies. Principal possibility of such effect was demonstrated for a number of basic proteins and peptides including cytochrome c [13,14], cardiotoxin II [15], poly-L-lysine [16], α-synuclein [17], to name only a few.

While membrane microdomain concept was put forward over four decades ago, it currently attracts increasingly growing attention because of several reasons. First, accumulating evidence substantiates significant role of membrane domains in a number of cellular events including signal transduction, coupling of G-proteins with their receptors, endo- or exocytosis, regulating the activity of phospholipase A_2, protein kinase C, modulating protein-membrane binding [18,19]. Second, recent very promising approach in molecular medicine, called membrane-lipid therapy considers membrane domains as a new target in the treatment of numerous human disorders including neurodegenerative, metabolic, autoimmune, infectious diseases, cancer, hypertension, etc. [20]. Third, a wealth of reports points to the strong correlation

* Corresponding author at: 19-32 Geroyev Truda St., 61144 Kharkov, Ukraine. Tel.: +38 057 268 41 49; fax: +38 057 343 82 44.
E-mail address: valtrusova@yahoo.com (V.M. Trusova).

0927-7765/$ – see front matter © 2010 Elsevier B.V. All rights reserved.
doi:10.1016/j.colsurfb.2010.06.011

between lateral phase separation and self-association propensities of lipid-bound proteins [21]. Particularly, membrane domains are believed to represent the nucleation sites for amyloid fibrils [22]. Finally, a number of experimental and theoretical works suggests that regardless their origin lipid domains may be the intermediate states of more complex membrane structures such as non-bilayer configurations, caveolae, coated pits, synaptosomes, etc. [23].

Notwithstanding the great progress that has been made over the past years, the factors, initiating and regulating domain formation as well as the exact molecular mechanisms behind lipid immiscibility, are still obscure. While establishing the correlation between protein-membrane association and lipid lateral redistribution, the model systems containing solid-supported lipid bilayers (SLBs) and isolated proteins prove to be extremely useful. In the present work we utilized total internal reflection fluorescence microscopy (TIRFM) to evaluate the ability of cationic protein lysozyme (Lz) to induce lateral redistribution of lipids in SLBs composed of zwitterionic lipid phosphatidylcholine (PC) and its mixtures with 5 or 25 mol% of anionic lipid cardiolipin (CL). The choice of this protein is dictated by the paramount physiological consequences of its association with membranes related not only to bactericidal, immunomodulatory and antitumor activities of lysozyme, but also by Lz propensity to convert into amyloid-like structures in a proper membrane environment. Lz-lipid interactions have been already placed in the focus of our research previously. Specifically, in the work [24] the formation of Lz oligomers in lipid environment upon increasing the membrane electrostatic surface potential has been reported, but the molecular level details of Lz-induced lipid bilayer structural perturbations remained beyond the scope of our research. In the work [25] we moved further, and explored the ability of Lz to induce lipid segregation using steady-state Förster resonance energy transfer (FRET). However, FRET is indirect method of detecting the alterations in lipid bilayer molecular architecture which can be interfered with another processes occurring in protein–lipid systems. TIRFM studies outlined here represent a direct real-time visualization of lipid bilayer morphology changes evoked by Lz, and thus may emerge more unambiguous picture of protein–lipid complexation.

2. Materials and methods

Egg yolk phosphatidylcholine and bovine heart cardiolipin were from Avanti Polar Lipids (Birmingham, AL). Hen egg lysozyme, HEPES and EDTA were purchased from Sigma (St. Louis, MO). 2-(4,4-Difluoro-5-methyl-4-bora-3a, 4a-diaza-s-indacene-3-dodecanoyl)-1-hexadecanoyl-sn-glycero-3-phosphocholine (BODIPY-PC) was from Invitrogen (Carlsbad, CA), 1-(1,2-diacylsn-glycero-3-phospho)-3-{1′-[7-(4,4-difluoro-1,3,5,7-tetramethyl-4-bora-3*a*, 4*a*-diaza-*s*-indacene-8-yl)heptanoyl]- 2′-acyl-*sn*- glycero-3 -phospho}glycerol (BODIPY-CL) was synthesized as described in detail elsewhere [26]. All other chemicals were of analytical grade and used without further purification.

2.1. Preparation of supported lipid bilayers

Lipid vesicles were made by extrusion technique from PC and its mixtures with 5 and 25 mol% CL [27]. Appropriate amounts of lipid stock solutions were mixed in chloroform, evaporated to dryness under a gentle nitrogen stream, and then left under reduced pressure for 1.5 h to remove any residual solvent. The dry lipid residues were subsequently hydrated with 20 mM HEPES, pH 7.4 at room temperature to yield lipid concentration of 1 mM. Thereafter, the sample was subjected to 15 passes through a 50 nm pore size polycarbonate filter (Millipore, Bedford, MA), yielding the liposomes of desired composition. BODIPY-PC or BODIPY-CL (0.3 mol% of total lipid, respectively) were added to the mixture of PC and CL prior to the solvent evaporation. SLBs were made by vesicle fusion [28]. Homemade chambers, consisting of a glass frame to which two coverslips are attached using silicon grease, were used for microscopy. Chambers were filled with liposome suspension containing 100 μM total lipid and 5 mM $CaCl_2$, the latter added immediately before the bilayer deposition. After incubation for 20 min in the dark, excess liposomes were thoroughly washed with working buffer. Immediately before bilayer formation, glass coverslips were cleaned by sonication for 30 min at 50 °C with detergent solution, rinsed with hot tap water, ethanol, and Milli-Q water. The slides and vesicles were used within 8 h after preparation. Hereafter, SLBs containing 5 or 25 mol% CL are referred to as CL5 or CL25.

2.2. Total internal reflection microscopy

To study membrane processes it is convenient to limit the observation to a very thin layer. The total internal reflection fluorescence (TIRF) technology allows limiting the observation depth below 200 nm. To study the fluorescence from supported bilayers we used inverted total internal reflection fluorescence microscope Olympus IX71 with argon ion laser as an excitation source (excitation wavelength was 488 nm). High-resolution imaging was carried out with an oil immersion Olympus 60X TIRFM objective. Fluorescence images were collected using Hamamatsu CCD camera interfaced to a computer and operated by Simple PCI software provided by camera manufacturer. Subsequent image processing was performed using ImageJ software.

3. Results

To explore the impact of Lz on surface topography of SLBs we used total internal reflection fluorescence microscopy. In the absence of protein, freshly formed lipid bilayers were characterized by even fluorescence with no evidence of any bilayer defects (panels A in Figs. 1–5). Addition of Lz to neat PC membranes exerted no influence on SLB morphology, as can be judged from invariance of BODIPY-PC fluorescence (Fig. 1B–D). Furthermore, PC SLBs were similarly homogeneous in appearance, with no obvious changes in bilayer organization even after 60 min of protein–lipid interactions (Fig. 1D). In contrast, in CL-containing lipid bilayers protein binding caused large well-defined areas with increased surface fluorescence of BODIPY-CL (cf. panels F in Figs. 2–5). These areas are of micrometer size, and in general remain in the plane of the SLB. These structures were not seen in control experiments in which plain buffer was added. The above findings suggest that the observed structures are lipid domains enriched in CL. These observations are in line with our recent studies in which the formation of domains rich in anionic lipids upon protein binding has been evidenced by FRET [25].

Lz-induced CL gathering into domains was found to be a function of three experimental variables: (i) anionic lipid content, (ii) Lz concentration, and (iii) time of Lz–lipid interactions (t). Analysis of the images with ImageJ software allowed extracting the quantitative parameters of domains (area, d, and occupation of the image field of view (FOV) by domains, σ). The recovered quantitative estimates, summarized in Table 1, suggest that elevating values of the above experimental variables lead to the increase in number and size of CL-replete areas. For the sake of exemplification, after 15 min of SLB exposure to 0.1 μM Lz (20:1 lipid/protein molar ratio, L:P) the value of σ in CL25 systems turned out to be 2.4-fold greater compared to CL5 bilayers (panel D in Figs. 2 and 3), while at protein concentration 0.4 μM (L:P = 5:1) this increment factor takes

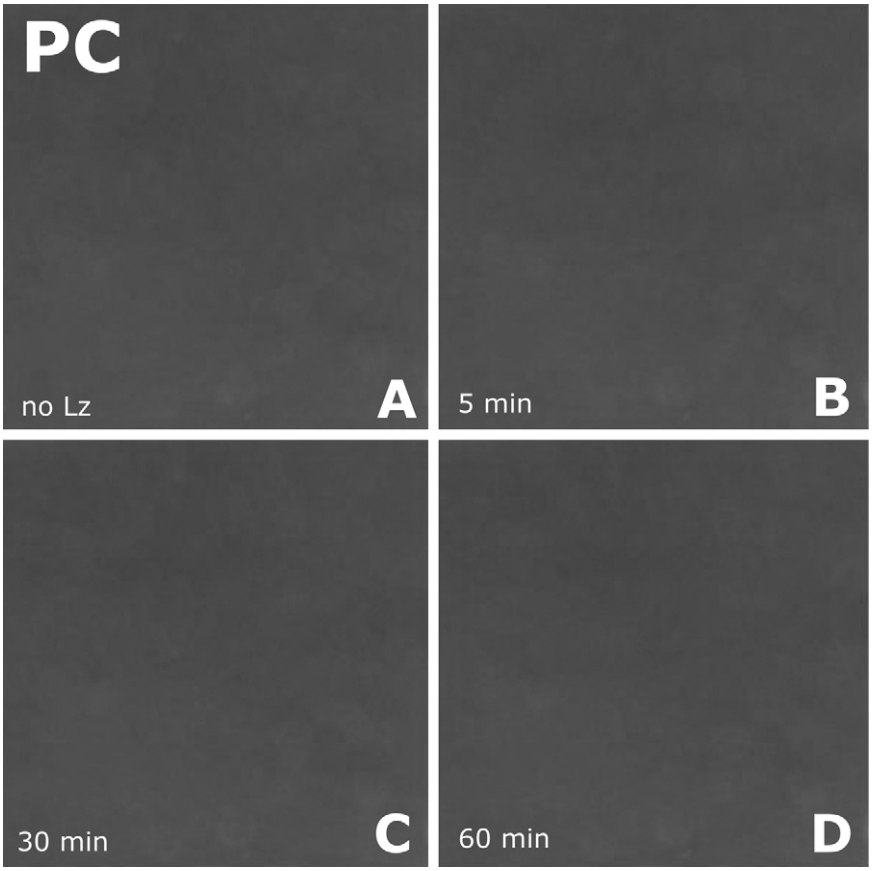

Fig. 1. TIRF microscopy images of PC bilayers in the absence (A) and presence (B–D) of lysozyme. Protein concentration was 0.4 μM, lipid/protein ratio was 5.

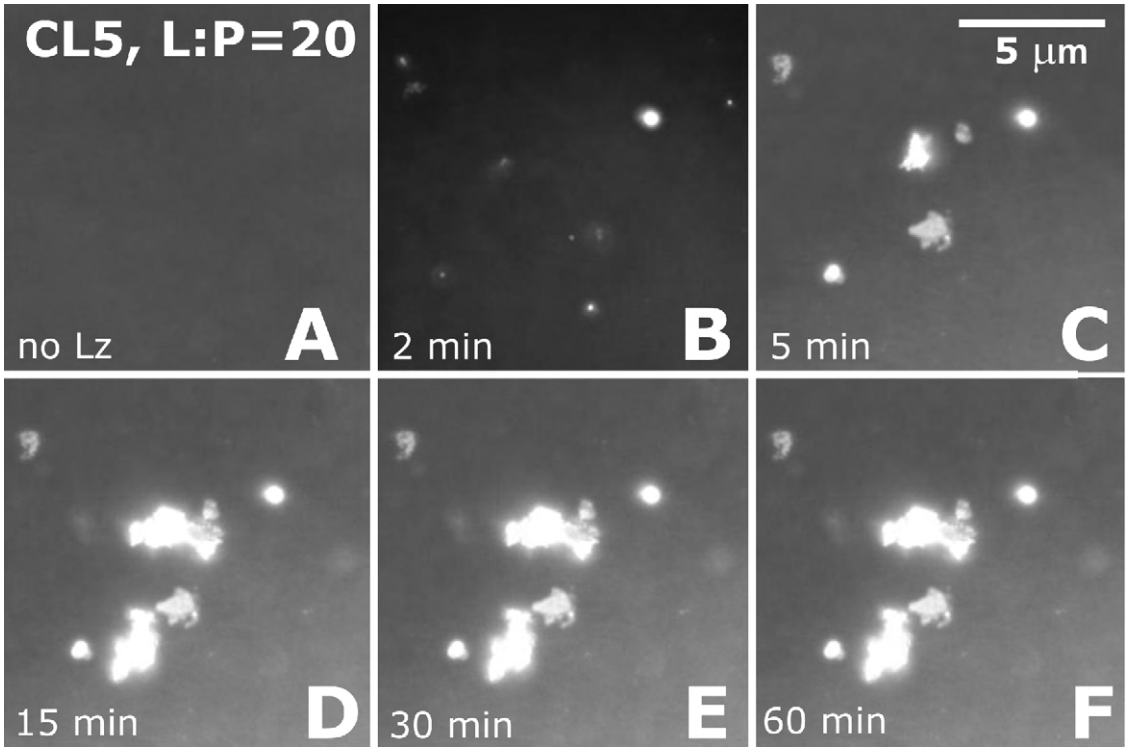

Fig. 2. Lysozyme-induced formation of CL domains in CL5 SLBs. The images were taken before (A) and after (B–F) the protein addition to yield a final lysozyme concentration of 0.1 μM.

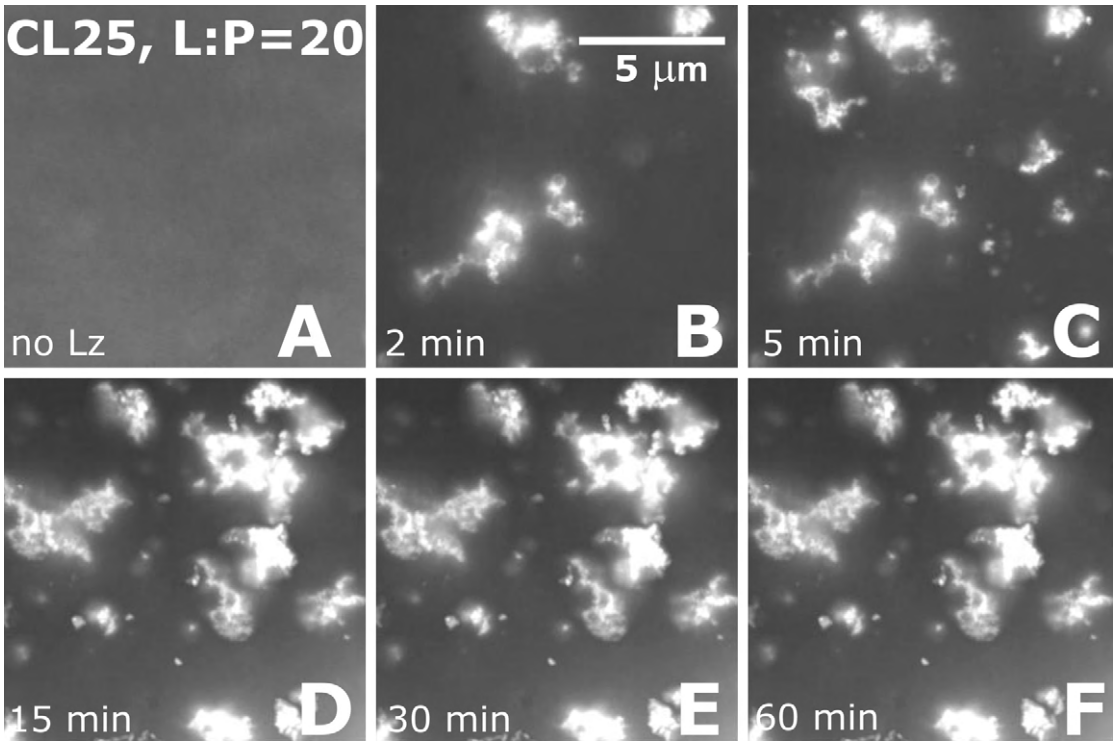

Fig. 3. Representative TIRFM image set of CL25 SLBs before (A) and after (B–F) their exposure to 0.1 μM of lysozyme.

the value of 3.7 (panel D in Figs. 4 and 5). To make sure that Lz itself does not contain any emitting moieties, increasing concentration of which could account for the observed expansion of bright spots, 0.4 μM Lz was incubated in working buffer over the glass substrate. It appeared that protein per second does not produce any fluorescent signal on the glass surface (data not shown). The above observations provide strong grounds for believing that the areas with increased surface fluorescence are induced exclusively by protein–lipid interactions. These areas seem to be formed by CL molecules assembling into domains upon Lz addition, because

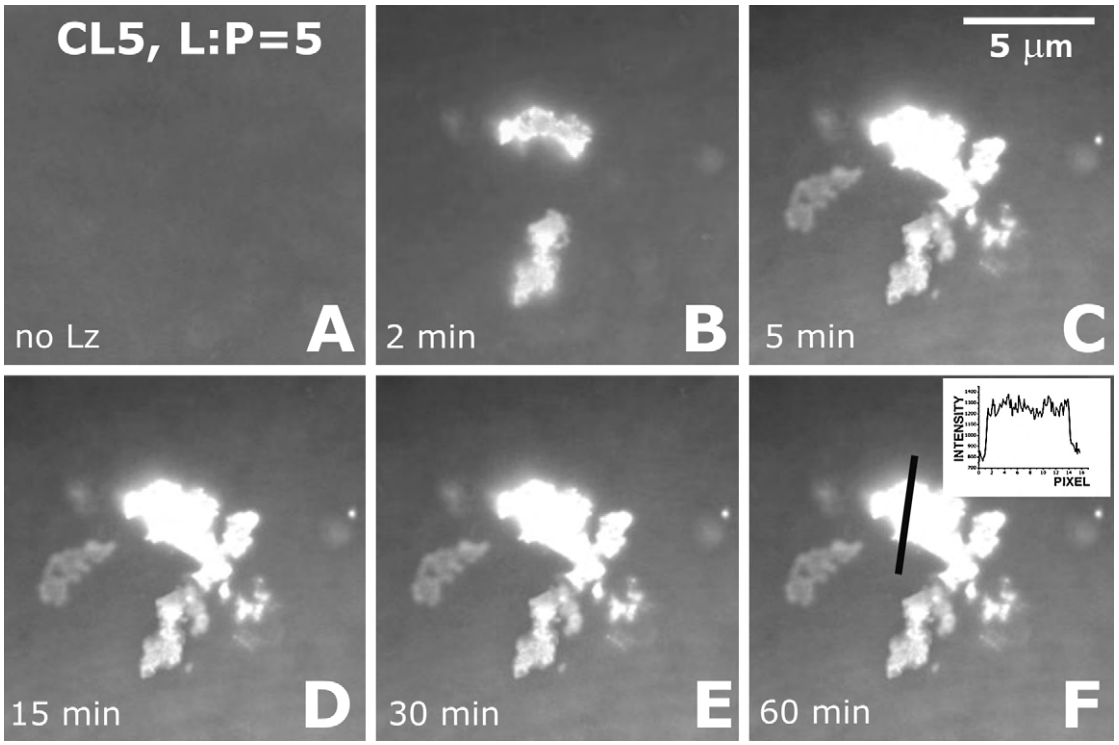

Fig. 4. Visualization of planar lipid domains formed upon lysozyme adsorption onto the surface of SLBs containing 5 mol% CL. Lipid/protein molar ratio was 5. The inset in panel F shows the intensity profile along the black line.

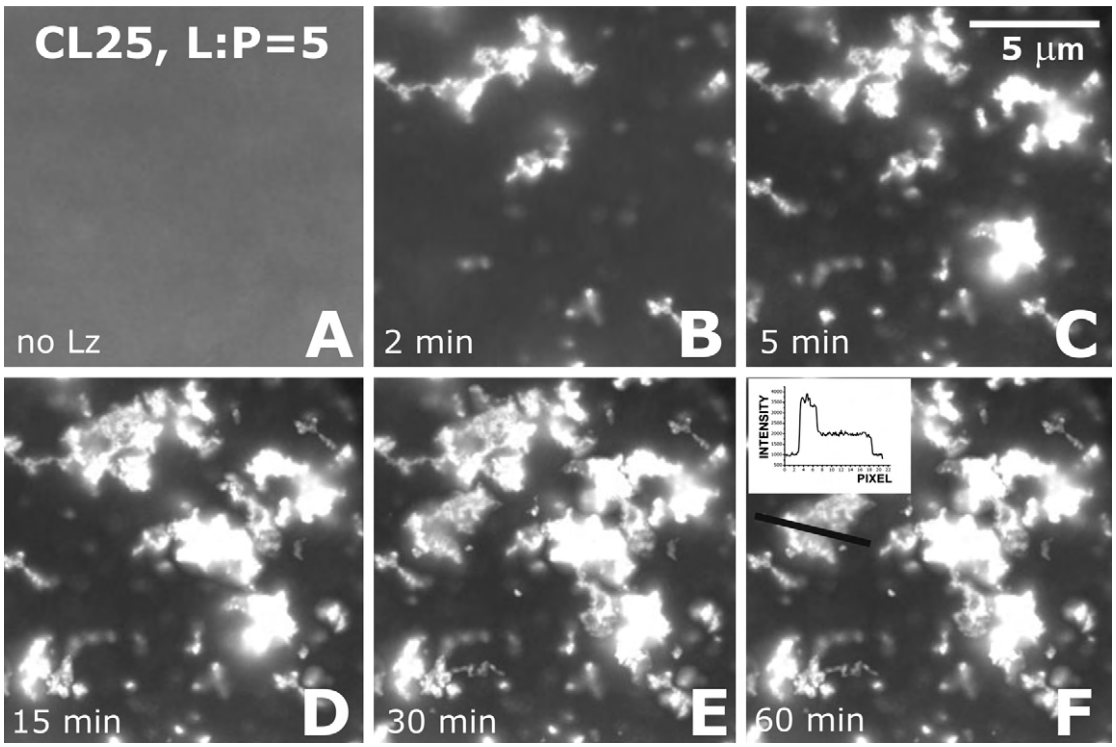

Fig. 5. Morphological changes in CL25 supported lipid bilayers provoked by lysozyme. Lipid/protein molar ratio was 5. The inset in panel F shows the intensity profile along the black line.

BODIPY-CL is the only fluorescing species excited by 488 nm laser source employed here.

Increasing time of protein incubation with SLBs also led to the nucleation and growth of lipid domains, area of which reached the maximum value of 21 μm^2 (CL25, L:P = 5:1, t = 15 min). Kinetic imaging of Lz–lipid mixtures revealed that gradual expansion of CL domains occurs over the time course of ~5 min for CL5 SLBs at L:P = 5:1 (Fig. 4C), ~30 min for CL25 bilayers at the same lipid/protein molar ratio (Fig. 5E), and ~15 min for the rest of systems (Figs. 2D and 3D). Thus, 2 min of 0.4 μM Lz interactions with CL25 bilayers result in ~10% occupation of image FOV by CL-enriched assemblies, while after 15 min of protein–lipid association this parameter (σ) was found to take the value of ~38% (panels B and D in Fig. 5, Table 1). Notably, the cessation time of CL domain growth is in a good agreement with our recent lipid monolayer studies which showed that time course of Lz-lipid binding (i.e. the time necessary for reaching the thermodynamic equilibrium) corresponds to 8 and 19 min for CL5 and CL25 monolayers, respectively, at L:P = 5:1, and to 7 and 14 min for the same systems at L:P = 20:1, respectively (V.M. Trusova, G.P. Gorbenko and P.K.J. Kinnunen, unpublished results).

Another noteworthy feature of the images is that at CL content 5 mol% the bright spots have more of less defined shape while in CL 25 bilayers these spots represent a sort of irregular network of highly fluorescent fluid regions being the most pronounced at L:P = 5 (Figs. 5D–F). The network seems to consist of bright regions embedded in a less fluorescent dark background which are characterized by a stepwise change in fluorescence intensity (Fig. 5F, inset). The step size between the areas of different intensity is discrete and approximately equals the intensity level of the parent bilayer (quantified after subtraction of camera noise). Intriguingly, intensity distribution profiles for CL5 SLBs were continuous, with brightness changes fluctuating around the average value (Fig. 4F, inset). This observation allowed us to put forward an idea that Lz induces the formation of planar domains in CL5 bilayers, and more complex structures such as multilayers folded from the parent bilayer and stacked on it in CL25 membranes. Interestingly, similar shape transformations were

Table 1
Structural parameters of lipid domains induced by lysozyme in supported lipid bilayers.

Lz concentration (μm)	t (min)	d[a] (μm^2)		σ (%)	
		CL5	CL25	CL5	CL25
0.1	2	0.17–1.2	0.18–3.5	1.9	3.7
	5	0.21–1.64	0.24–5.2	3	10
	15	0.32–7.75	0.4–9.04	6.9	16.6
	30	0.32–7.75	0.4–9.04	6.9	16.6
	60	0.32–7.75	0.4–9.04	6.9	16.6
0.4	2	0.3–4.84	0.31–8.96	4.3	9.8
	5	0.34–18.6	0.34–12.2	10.4	18.7
	15	0.34–18.6	0.34–21.4	10.4	38.18
	30	0.34–18.6	0.34–21.4	10.4	38.18
	60	0.34–18.6	0.34–21.4	10.4	38.18

[a] The figures correspond to the lower and upper limits of domain area (d) recovered for a given system.

observed upon interactions of surfactant proteins B and C with lipid monolayers [29,30].

4. Discussion

Lipid bilayer, a basic structural element of cell membranes, is a highly flexible material capable of deforming into diverse shapes. In cells, the lipid bilayer is highly heterogeneous and known to contain numerous ordered protein and lipid domains. Proteins are often required to guide the deformation of cellular membranes, and induce structural rearrangement and assembling of one or another membrane component driven by a spectrum of protein–lipid interactions ranging from van der Waals and steric interactions of protein transmembrane segment with lipid hydrophobic tails to electrostatic attraction or hydrogen-bonding between amino acid side chains and lipid headgroups [8–14]. Specifically, intrinsic membrane proteins may give rise to surface structuring of a lipid bilayer according to hydrophobic mismatch principle—when the polypeptide hydrophobic span exposed to the lipids does not match the length of acyl chain, the protein performs a sorting of lipids in such a way, that those lipid species providing the best hydrophobic fit would be crowding around the protein [9,31]. In turn, lipid demixing induced by extrinsic water-soluble proteins has predominantly electrostatic origin and is dictated by minimization of the electrostatic free energy of protein–lipid system [11,14,21]. The ultimate goal of the present work was to explore the impact of small polycationic protein lysozyme possessing a wide range of antimicrobial, antitumor and immunomodulatory activities, on the surface morphology of solid-supported lipid bilayers of different composition. Our TIRFM studies revealed remarkable differences in Lz interactions with neat PC and PC/CL bilayers. Protein binding to the neutral SLBs had no impact on lipid bilayer structure, as can be judged from invariance in TIRFM images over 60 min. Since a good deal of works indicate that Lz does bind to PC bilayers [24,32,33], our findings may suggest that either the protein has no influence on molecular organization of this type of SLBs, or the perturbations induced by Lz are below optical resolution. Dramatically different behavior was observed for CL-containing lipid bilayers where protein sorption brought about the formation of lipid domains enriched in anionic lipid identified in microscopy images as large areas with increased surface fluorescence. The fact that the size and number of these areas tend to increase with CL content pinpoints the electrostatic protein–lipid interactions as initial driving force of lipid demixing. Comprehensive results from a vast number of theoretical and experimental studies emerge a mechanism according to which the fluid nature of lipid bilayer allows the lipid constituent with the higher protein affinity to migrate laterally towards the interaction zone, locally modulating the lipid composition. The factors facilitating the preferential interactions of basic proteins with anionic lipids can be outlined as follows [3]:

(a) The presence of clusters of positively charged amino acid residues on the protein surface allowing one protein molecule to interact simultaneously with several anionic lipids.
(b) Conformational flexibility of a polypeptide chain favoring the formation of protein conformer in which the distance between amino acid positive charges and anionic lipid headgroups would be minimal.

In fundamental works of Ibrahim et al. a specific helix-loop-helix (HLH) domain (residues Asp_{87}–Arg_{114}) located at the upper lip of Lz active site and responsible for protein-membrane binding, has been identified [34,35]. Based on these results, in our previous paper we proposed tentative disposition of Lz relative to lipid–water interface [24]. According to our model, Lz adsorbs onto lipid bilayer with its long axis being parallel to membrane surface. In such an orientation, protein side, facing the bilayer upon binding, contains the cluster of positively charged amino acids embracing the residues Lys_{13}, Arg_{14}, Arg_{21}, Lys_{96}, Lys_{97}, and Arg_{114}. Furthermore, based on the results of computer modeling, Saburova et al. showed that Lz has long extended regions with positive potential, and the rupture of these regions occurs only at pH > 8 [36]. Lz is a polycationic protein with isoelectric point of $pI \sim 11$. The number of Lz basic groups twice as large as the number of anionic ones, and the highest value of pK_a is attributed to Glu_{35} ($pK_a \sim 6.2$) [37]. The distribution of electrostatic potential on protein surface is determined by microenvironment of special amino acid residues. Specifically, it was shown that the shift of Glu_{35} and Asp_{52} pK_a towards the acidic values results in the 1.5-fold decrease in the number of regions with positive potential at pH 4, and exerts no effect in pH range from 4 to 8 [36]. In the active site of the protein where the magnitude of electric field is estimated to be 12×10^{-6} V/cm^2, there exists the gradient between positive and negative equipotential surfaces [38]. The areas of protein cationic clusters range from 1.12 to 3.4 nm^2, while area of lipid polar headgroup is $\leq$0.65 nm^2. To minimize the energy cost associated with the binding of such highly charged protein patches, lipids must reorganize to create zones of elevated local CL concentration. This rearrangement produces the gradients in bilayer electrostatic potential profile (or "polarization") faded as the distance from protein binding site increases [12]. Electrostatic nature of CL accumulation in the immediate vicinity of adsorbed Lz could readily account for our observation that domain size and number increases with protein concentration and anionic lipid content—the more protein is initially available for membrane binding, the more positive charges can be compensated and the larger areas of negatively charged lipid are required. Inversely, increasing amounts of CL would attract more protein for binding thereby enhancing the demixing process.

However, as evidenced from our results, the formation of planar domain does not terminate Lz-evoked membrane deformation when CL molar fraction reaches the value of 25 mol%. More specifically, the facts that in this type of SLBs (i) lipid domains resemble the irregular network in which one monolayer superimposes on another one, and (ii) intensity profiles have discrete character, raise at least two questions: a) whether Lz is capable of inducing more complex structures such as lipid multilayer stacks, and b) what factors control the switch between in-plane lipid domains and more complex assemblies. The answer to the first question can be found while considering lysozyme as antimicrobial polypeptide. Several lines of evidence suggest that Lz induces the damage of bacterial membrane via "carpet" mechanism [34,35,39]. Briefly, this mechanism implies that Lz amphipatic α-helices constituting the HLH domain, once adsorbed onto bilayer surface accumulate around themselves anionic lipids thus locally changing membrane curvature and composition. In the site of binding (i.e. within the region of increased concentration of anionic lipids) protein generates the lateral pressure on the membrane, causing in such a fashion its invagination. This results in membrane thinning (Fig. 6, right) and uptaking of a part of lipid molecules from the bilayer, followed by membrane deformation, defragmentation and micellization [40]. Evidently, with some exceptions, the sequence of the events in our systems is quite similar. Lz attaches to the headgroups of anionic CL via electrostatic attraction giving rise to the lateral migration of CL molecules, remote from protein binding site, towards the interaction zone. Clustering of CL creates the gradients of curvature and line tension along the membrane surface. The formation of in-plane domains finishes the global membrane perturbations induced by Lz in CL5 SLBs (Fig. 6, right). However, if the curvature radius of anionic lipid-enriched areas significantly exceeds that of surrounding lipids, membrane can further lower the interaction energy by bending and stretching [3]. While elec-

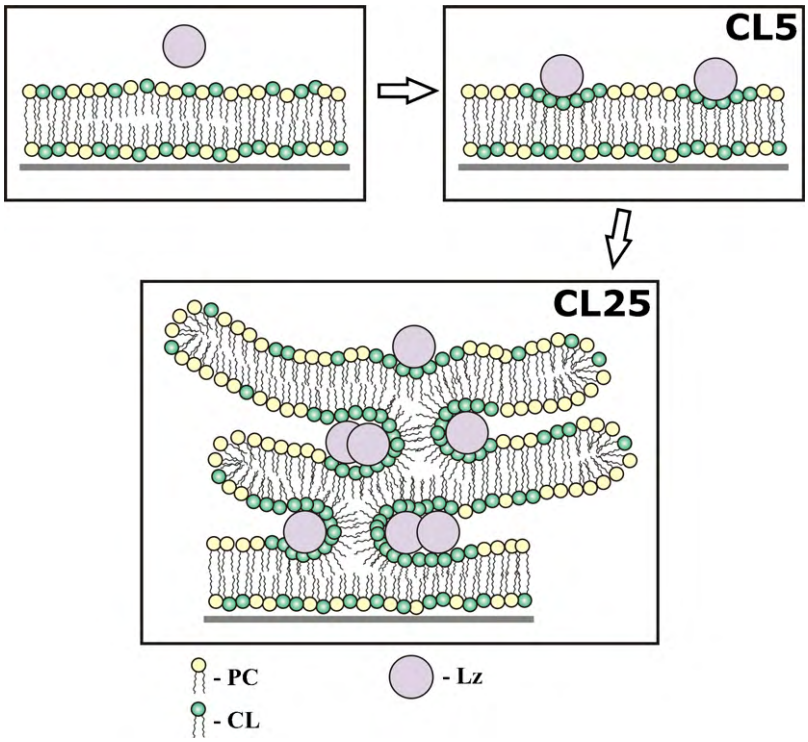

Fig. 6. Schematic representation of planar domain formation and multilayer stacking in supported lipid bilayers in response to lysozyme sorption.

trostatic protein–lipid interactions underlie the initial crowding of specific lipids around the adsorbate, the elasticity of membrane dictates further possible structural transformations of CL-segregated regions in CL25 bilayers. In contrast to classical "carpet" model, in our systems such transformation may manifest itself in squeezing out the multilayer lipid stacks from parent SLB. These stacks represent the sheets of lipid bilayers homogeneously stacked on the top of each other and separated by protein molecules (Fig. 6, bottom). Importantly, in stacking geometry electrostatic free energy of protein-membrane binding is likely to reach its minimum because all lipid charges are in contact with protein charges, while in lamellar phase only a fraction of anionic lipids is vicinal to Lz (Fig. 6, bottom). This tentative mechanism is in good agreement with the idea of Coutinho et al. [41] who proposed "pinched lamellar" model for Lz/lipid aggregates. According to this model, Lz induces cross-linking of lipid bilayers through multiple protein–protein bridges in the places where anionic lipid domains are formed. Based on the results of comprehensive resonance energy transfer studies, the authors calculated that lamellar repeat distance is ~5–7 nm while the separation of the regions between these "pinched structures" containing large pockets of water which are stabilized by hydration repulsion, corresponds to ~9–10.5 nm.

Yet, our multilayer stacking scenario does not readily explain why this kind of lipid protrusions is observed only in CL25 bilayers. In an attempt to define the factors responsible for the transformation of planar domains into bilayer stacks (Fig. 6), we addressed to our previous study on Lz adsorption onto the negatively charged lipid bilayers [24]. Specifically, using different modifications of steady-state fluorescence spectroscopy, we found that at low CL content (<11 mol%) Lz exists in membrane environment as monomer. However, upon increasing molar fraction of CL up to 25 mol%, the formation of protein aggregates between bilayer-bound Lz molecules occurs. If this is the case, then protein oligomers would enhance demixing potential of CL, and trigger the formation of anionic lipid assemblies with higher radius of curvature compared to monomer-induced domains. Apparently, under the conditions of elevated negative curvature strain, imposed by Lz, in-plane domains cannot provide the minimal free energy of the composite protein–lipid membrane, and the route by which the system further reduces the interaction energy seems to involve transformation of regular domains into multilayer stacks. In CL5 SLBs, due to initially lower degree of demixing, the transition into 3D geometry is not required for reaching a thermodynamic equilibrium, and planar domains enriched in either CL or PC represent the most stable membrane conformation.

Taken together, the results presented here clearly demonstrate that Lz impact on lipid bilayer organization can be controlled by the membrane surface charge density. As follows from our TIRFM studies, the formation of planar CL domains is characteristic of the protein binding to the weakly charged CL5 SLBs, while at higher CL content (25 mol%), in accord with energy minimization principle, these domains are able to convert into multilamellar lipid stacks. The ability of Lz to induce lipid lateral segregation may underlie its antimicrobial action and denote the mechanism of bacterial membrane disruption arising from the formation of packing irregularities at the locations, where the two phases (enriched either in neutral or anionic lipids) become juxtaposed. An attractive feature of this mechanism is that it can be used to rationally design Lz-based antimicrobial agents with toxicity selective for certain organisms. In turn, the biological relevance of multilayer stacks representing large surface-confined reservoirs is enigmatic at this stage, but seems to involve at least two implications. The first one is related to the membrane-assisted conversion of Lz oligomers into amyloid-like structures—highly ordered fibrillar pathological aggregates associated with a number of so-called conformational diseases (Parkinson's, Alzheimer's and Huntington's diseases, type II diabetes, spongiform encephalopathies, systemic amyloidosis) [42]. Assuming that the separation distance between lipid layers is close to protein diameter, these surface-confined reservoirs may serve as pockets for crowding of protein monomeric species and formation of nuclei for amyloid fibrils. Second, these complexes may represent novel protein–lipid-based drug delivery systems

where drug is entrapped into the water pockets, while lysozyme ensures the proper targeting.

5. Conclusions

Cumulatively, using total internal reflection fluorescence microscopy we have analyzed the formation of CL-enriched areas induced by the adsorption of Lz onto PC/CL supported lipid bilayers under varying experimental conditions. The key findings are:

- Lz binding to SLBs evokes the segregation of lipid bilayer components and the formation of CL-enriched areas with their number and size being dependent on: (i) anionic lipid content; (ii) Lz concentration; and (iii) time of Lz-lipid interactions;
- at CL content 5 mol% formation of planar domains enriched either in PC or CL represents the finite stage of Lz-evoked membrane deformation;
- at higher molar fraction of CL (25 mol%) these in-plane domains transform into multilamellar lipid stacks according to energy minimization principle.

Acknowledgements

This work was supported by the grant no. 4534 from the Science and Technology Center in Ukraine, grant no. F28.4/007 from Fundamental Research State Fund, grant NIH EB012334 (to Z.G.), grant from European Social Fund (project number 2009/0205/1DP/1.1.1.2.0/09/APIA/VIAA/152) and grant 09-04-00313 of Russian Foundation for Basic Research. VT gratefully acknowledges an award by Human Frontier Science Program.

References

[1] S.J. Singer, G.L. Nicholson, Science 175 (1972) 720–731.
[2] P.K.J. Kinnunen, Chem. Phys. Lipids 57 (1991) 375–399.
[3] S. Mukherjee, F.R. Maxfield, Annu. Rev. Cell Dev. Biol. 20 (2004) 839–866.
[4] W.H. Binder, V. Barragan, F.M. Menger, Angew. Chem. Int. Ed. 42 (2003) 5802–5827.
[5] O.G. Mouritsen, K. Jørgensen, Chem. Phys. Lipids 73 (1994) 3–25.
[6] K. Simons, W.L.C. Vaz, Annu. Rev. Biophys. Biomol. Struct. 33 (2004) 269–295.
[7] M. Edidin, Annu. Rev. Biophys. Biomol. Struct. 32 (2003) 257–283.
[8] D. Marsh, Mol. Membr. Biol. 12 (1995) 59–64.
[9] A. Hinderliter, R.L. Biltonen, P.F. Almeida, Biochemistry 43 (2004) 7102–7110.
[10] E.C. Mbamala, A. Ben-Shaul, S. May, Biophys. J. 88 (2005) 1702–1714.
[11] T. Heimburg, B. Angerstein, D. Marsh, Biophys. J. 76 (1999) 2575–2586.
[12] G. Denisov, S. Wanaski, P. Luan, M. Glaser, S. McLaughlin, Biophys. J. 74 (1998) 731–744.
[13] D. Haverstick, M. Glaser, Biophys. J. 55 (1989) 677–682.
[14] G.P. Gorbenko, V.M. Trusova, J.G. Molotkovsky, P.K.J. Kinnunen, Biochim. Biophys. Acta 1788 (2009) 1358–1365.
[15] M.A. Carbone, P.M. Macdonald, Biochemistry 35 (1996) 3368–3378.
[16] C.M. Franzin, P.M. Macdonald, Biophys. J. 81 (2001) 3346–3362.
[17] A.P. Pandey, F. Haque, J.C. Rochet, J.S. Hovis, Biophys. J. 96 (2009) 540–551.
[18] J.C.M. Holthuis, G. Vanmeer, K. Huitema, Mol. Membr. Biol. 20 (2003) 231–241.
[19] T. Kobayashi, Y. Hirabayashi, Glycoconj. J. 17 (2000) 163–171.
[20] P.V. Escriba, J.M. Gonzales-Ros, F.M. Goni, P.K.J. Kinnunen, L. Vign, L. Sanchez-Magraner, A.M. Fernandez, X. Busquets, I. Horvath, G. Barcelo-Coblijn, J. Cell Mol. Med. 12 (2008) 829–875.
[21] S. May, D. Harries, A. Ben-Shaul, Biophys. J. 79 (2000) 1747–1760.
[22] W.G. Wood, F. Schroeder, U. Igbavboa, N.A. Avdulov, S.V. Chochina, Neurobiol. Aging 23 (2002) 685–694.
[23] R. Lipowsky, R. Dimova, J. Phys.: Condens. Mater. 15 (2003) S31–S45.
[24] G.P. Gorbenko, V.M. Ioffe, P.K.J. Kinnunen, Biophys. J. 93 (2007) 140–153.
[25] G.P. Gorbenko, V.M. Ioffe, J.G. Molotkovsky, P.K.J. Kinnunen, Biochim. Biophys. Acta 1778 (2008) 1213–1221.
[26] I.A. Boldyrev, X. Zhai, M.M. Momsen, H.L. Brockman, R.E. Brown, J.G. Molotkovsky, J. Lipid Res. 48 (2007) 1518–1532.
[27] B. Mui, L. Chow, M.J. Hope, Meth. Enzymol. 367 (2003) 3–14.
[28] R. Richter, A. Mukhopadhyay, A. Brisson, Biophys. J. 85 (2003) 3035–3047.
[29] S. Krol, M. Ross, M. Sieber, S. Kunneke, H.J. Galla, A. Janshoff, Biophys. J. 79 (2000) 904–918.
[30] A. von Nahmen, A. Post, H.J. Galla, M. Sieber, Eur. Biophys. J. 26 (1997) 359–369.
[31] J.A. Killian, Biochim. Biophys. Acta 1376 (1998) 401–415.
[32] V.M. Ioffe, G.P. Gorbenko, Biophys. Chem. 114 (2005) 199–204.
[33] H.K. Kimelberg, Mol. Cell Biochem. 10 (1976) 171–190.
[34] H.R. Ibrahim, M. Yamada, K. Matsushita, K. Kobayashi, A. Kato, J. Biol. Chem. 269 (1994) 5053–5063.
[35] H.R. Ibrahim, U. Thomas, A. Pellegrini, J. Biol. Chem. 276 (2001) 43767–43774.
[36] E.A. Saburova, Yu.N. Dybovskaya, N.V. Avseenko, V.S. Sivozhelezov, Proc. XII Int. Conf. “Mathematics. Computer Education” vol. 3, Izhevsk, 2005, pp. 923–933.
[37] V.Z. Spassov, L. Yan, Protein Sci. 17 (2008) 1955–1970.
[38] S. Dao-Pin, D.I. Liao, S.J. Remington, Proc. Natl. Acad. Sci. 86 (1989) 5361–5365.
[39] H.N. Hunter, W. Jing, D.J. Schibli, T. Trinha, Y. Park, S.C. Kim, H.J. Vogel, Biochim. Biophys. Acta 1668 (2005) 175–189.
[40] M.R. Yeman, N.Y. Yount, Pharmacol. Rev. 55 (2003) 27–55.
[41] A. Coutinho, L.M.S. Loura, A. Fedorov, M. Prieto, Biophys. J. 95 (2008) 4726–4736.
[42] C.M. Dobson, Philos. Trans. Soc., Lond. Ser. B 356 (2001) 133–145.